

Diffusion-weighted imaging of breast tumours at 3 Tesla and 7 Tesla: a comparison

S. Gruber^{1,2} · L. Minarikova^{1,2} · K. Pinker³ · O. Zaric^{1,2} · M. Chmelik^{1,2} · B. Strasser^{1,2} · P. Baltzer³ · T. Helbich³ · S. Trattnig^{1,2} · W. Bogner^{1,2}

Received: 9 March 2015 / Revised: 13 July 2015 / Accepted: 27 July 2015 / Published online: 27 August 2015
© European Society of Radiology 2015

Abstract

Objectives To compare bilateral diffusion-weighted MR imaging (DWI) at 3 T and 7 T in the same breast tumour patients. **Methods** Twenty-eight patients were included in this IRB-approved study (mean age 56±16 years). Before contrast-enhanced imaging, bilateral DWI with $b=0$ and 850 s/mm² was performed in 2:56 min (3 T) and 3:48 min (7 T), using readout-segmented echo planar imaging (rs-EPI) with a 1.4×1.4 mm² (3 T)/0.9×0.9 mm² (7 T) in-plane resolution. Apparent diffusion coefficients (ADC), signal-to-noise (SNR) and contrast-to-noise ratios (CNR) were assessed. **Results** Twenty-eight lesions were detected (18 malignant, 10 benign). CNR and SNR were comparable at both field strengths ($p>0.3$). Mean ADC values at 7 T were 4–22 % lower than at 3 T ($p\leq 0.03$). An ADC threshold of 1.275×10^{-3} mm²/s resulted in a diagnostic specificity of 90 % at both field strengths. The sensitivity was 94 % and 100 % at 3 T and 7 T, respectively. **Conclusion** 7-T DWI of the breast can be performed with 2.4-fold higher spatial resolution than 3 T, without significant differences in SNR if compared to 3 T.

Key points

- 7 T provides a 2.4-fold higher resolution in breast DWI than 3 T
- 7 T DWI has a high diagnostic accuracy comparable to that at 3 T
- At 7 T malignant lesions had 22 % lower ADC than at 3 T ($p<0.001$)

Keywords Breast MRI · Breast cancer · 7 Tesla · DWI · Diffusion

Introduction

Dynamic contrast-enhanced (DCE) magnetic resonance imaging (MRI) in breast cancer has developed into a powerful clinical tool for the characterization and detection of malignant and benign breast tumours. This and the morphologic appearance of lesions on contrast-enhanced MRI provide an exceptional sensitivity of up to 100 % for detection of breast cancer [1–6], and a specificity not less than 80 % which has been illustrated at different field strengths (1.5, 3 or 7 T) presuming that correct techniques and experienced readers are available [7–9].

To further increase the diagnostic specificity of breast MR imaging, supplementary MR methods, in particular, diffusion-weighted imaging (DWI), were proposed for inclusion into clinical MR imaging protocols for breast cancer diagnosis [10–12]. DWI is one of the most promising adjunct MRI methods. It probes the tissue microstructure by quantifying restricted water diffusion, resulting in an additional quantitative marker—the apparent diffusion coefficient (ADC)—to distinguish between benign and malignant lesions or to monitor treatment success [13–15].

At low magnetic fields (e.g. 1.5 T), DWI suffers from low spatial resolution. Higher magnetic fields (i.e. 3 T and above)

✉ S. Trattnig
siegfried.trattnig@meduniwien.ac.at

¹ MRCE, Department of Biomedical imaging and Image-Guided Therapy, Medical University Vienna, Lazarettgasse 14, 1090 Vienna, Austria

² Christian Doppler Laboratory for Clinical Molecular MR Imaging, Vienna, Austria

³ Division of Molecular and Gender Imaging, Department of Biomedical imaging and Image-Guided Therapy, Medical University Vienna, Vienna, Austria

offer increased signal-to-noise ratio (SNR) that can be translated into higher spatial resolution [16]. This could improve differentiation of benign and malignant lesions based on ADC values. Matsuoka et al. compared DWI in breast cancer between 1.5 T and 3 T in 13 patients [17]. They found no differences in ADC values at 1.5 and 3 T. For large lesions there was no difference in image scores between the two field strengths. In contrast, better image scores and improved lesion visibility for small lesions at 3 T, compared to 1.5 T, were reported. Initial breast MRI studies exploring ultra-high fields (7 T) provided evidence of substantially improved image quality compared to lower field strengths [18].

Promising unilateral breast DWI results from three patients [19] and a volunteer [20] were also reported at 7 T. An up to 5.7-fold SNR increase, compared to 3 T, was found with the same imaging parameters, but the spatial resolution and image quality were hampered by the use of single shot echo planar imaging (ss)-EPI, fat suppression failure and motion artefacts [19]. Recent results at 3 T and 7 T obtained in the brain and in the breast indicate that readout-segmented (rs)-EPI combined with parallel imaging improves image quality substantially and is able to overcome former restrictions in spatial resolutions at ultra-high B_0 [21–23]. Recently, Bogner et al. showed that rs-EPI improves the diagnostic performance of diffusion-weighted MR breast examinations at 3 T compared to ss-EPI [11]. Moreover, the use of rs-EPI enables DWI at ultra-high fields with reduced distortions but increased measurement time compared to ss-EPI.

A direct comparison of contrast-enhanced breast MRI between 3 T and 7 T showed excellent diagnostic accuracy at both field strengths, and comparable SNR when using a 3.2-fold higher spatial resolution at 7 T, compared to 3 T [9].

International guidelines recommend the use of an in-plane resolution of $1 \times 1 \text{ mm}^2$ or less for clinical contrast-enhanced breast MRI at 1.5 T [24]. However, at 1.5 T DWI is usually measured with lower resolution. Recently, a relatively high in-plane resolution of $1.1 \times 1.1 \text{ mm}^2$ in breast DWI using a special zoom-in technique was reported at 1.5 T [25].

The increased SNR at 7 T in breast MRI and DWI, compared to that at 3 T, can be translated into even higher spatial resolution [9, 19]. A spatial resolution comparable to clinical DCE MRI could improve the morphological evaluation of breast lesions based on DWI, in addition to ADC quantification at 7 T.

The purpose of this study was to compare bilateral breast DWI at 7 T with $0.9 \times 0.9 \text{ mm}^2$ in-plane resolution with breast DWI at 3 T with $1.4 \times 1.4 \text{ mm}^2$ in-plane resolution in the same breast tumour patients.

Materials and methods

The local ethics committee approved this study. Inclusion criteria for enrolment in this study were 18 years or older;

not pregnant or breastfeeding; no contraindication to MR imaging or contrast agents; no previous treatment; clinical indication for MRI of the breast; clinical abnormality or suspicious finding on mammography or breast ultrasound (asymmetric density, architectural distortion or breast mass classified according to the Breast Imaging Reporting and Data System, BI-RADS). In premenopausal women, MRI was performed between day 7 and 14 of the menstrual cycle.

Twenty-nine patients who were referred from our breast clinics with either suspicious clinical findings or mammographically and/or sonographically detected abnormalities were included in this study.

They were measured consecutively between April and November 2012 on both a 3 T Tim Trio and a 7 T Magnetom MR system (both Siemens Healthcare, Erlangen, Germany) within 4 days using dedicated bilateral breast coils with four ^1H channels (3 T: In vivo, Orlando, FL, USA; 7 T: $^1\text{H}/^31\text{P}$ coil, H. Stark, Erlangen, Germany) in the prone position. One patient was excluded from the study because of inadequate fat saturation, caused by a B_0 shimming failure at 7 T. Therefore, in this study 28 patients, 55 ± 16 years old (mean \pm SD, age range 23–81), were included. Written, informed consent was obtained from all patients prior to MR imaging.

Lesions were either histopathologically verified by image-guided breast biopsy ($n=8/28$) or by surgery ($n=18/28$; surgical biopsy, mastectomy or lumpectomy). Clinical and imaging follow-up was performed for more than 2 years in two patients who did not undergo surgery or biopsy ($n=2/28$; both classified as BI-RADS 3 with DCE MRI at 3 T).

Data acquisition

Bilateral three-direction trace DWI was performed with similarly adjusted sequence parameters in 2:56 min (3 T) and 3:48 min (7 T) using combined rs-EPI with fat-suppression and with b values of 0 and 850 s/mm^2 , suggested previously (Table 1) [10]. To make full use of the hardware at both MR scanners, the in-plane resolution ($1.4 \times 1.4 \text{ mm}^2$ at 3 T and $0.9 \times 0.9 \text{ mm}^2$ at 7 T) was adjusted to the best possible at both field strengths to compensate for the expected increase in SNR at 7 T (i.e. $7/3=2.3$). The slice thickness (5 mm) was identical. The measured field of view was 320×160 and the number of slices was 28. To allow a higher resolution at 7 T without causing additional blurring and distortions (i.e. same echo spacing of 0.32 ms), we used nine readout segments at 7 T compared to five at 3 T in combination with parallel imaging resulting in comparable effective TEs (62 ms vs 68 ms at 3 T vs 7 T).

DCE MRI was performed using a T_1 -weighted 3D time-resolved angiography with stochastic trajectories (TWIST) sequence using intravenously injected contrast as a bolus (0.2 mL/kg of body weight) after three baseline images, as described previously [9, 26].

Table 1 Sequence parameters for 3 T and 7 T DWI

Parameter	3 T	7 T
Diffusion directions	3 – scan trace	3 – scan trace
Diffusion schema	Stejskal–Tanner	Stejskal–Tanner
<i>b</i> values (s/mm ²)	0, 850	0, 850
Fat suppression	Frequency-selective and gradient reversal	Frequency-selective and gradient reversal
Refocusing	Low SAR	Low SAR
Repetition time (ms)	5800	5500
Echo time (ms)	68	62
Matrix size	256×128	340×170
Field of view (mm ²)	360×180	320×160
Number of averages	1	1
Voxel size (mm ³)	1.4×1.4×5	0.9×0.9×5
Slices per slab	28	28
Slice thickness (mm)	5	5
Readout segments	5	9
Parallel imaging	–	GRAPPA, factor 2
Acquisition time (min)	2:54	3:48

Data evaluation and statistical analysis

During post-processing, two-dimensional regions of interest (ROIs) were drawn manually in the lesion and in homogeneous breast parenchyma without enhancement (in the contralateral breast) in three different parts of the breast, namely para-mammillar, central and pre-pectoral, using OsiriX® (Pixmeo, Geneva, Switzerland) software by two readers in consent (radiologists with more than 7 years of experience in DWI of the breast; trained at different institutions).

The ROIs were drawn on the diffusion-weighted ($b=850$ s/mm²) images. The slice with the largest diameter of the lesion was used. Necrotic areas, represented as hyperintense regions on both diffusion-weighted ($b=850$ s/mm²) and ADC maps, were excluded. SNR was defined as the ratio between mean signal amplitude inside the ROI (S_{ROI}) and standard deviation of the background noise (σ_{BG}) ($SNR=S_{ROI}/\sigma_{BG}$). Contrast-to-noise (CNR) ratio was calculated as the difference between S_{ROI} and signal amplitude in tissue (ST), divided by the standard deviation in the lesion ROI (σ_{ROI}) and normal tissue ROI (σ_T).

$$CNR = \frac{S_{ROI} - S_T}{\sqrt{\sigma_{ROI}^2 + \sigma_T^2}}$$

A logarithmic transformation was performed on the skewed SNR data to achieve data normality. Mean ADC, CNR and transformed SNR values were calculated. They were compared using a two-way analysis of variance (ANOVA) for repeated measures in the case of SNR and ADC data from healthy tissue, because more than one value from one patient was used (three healthy tissue ROIs) and a

paired *t* test was used for ADC, SNR and CNR means comparison of ROIs from malignant and benign lesions. The 95 % confidence intervals of the diagnostic sensitivity, specificity, positive predictive value and negative predictive value were calculated with ADC threshold of 1.275×10^{-3} mm²/s, established previously for similar diffusion imaging parameters in a larger patient study ($n=247$ patients) at 3 T [27]. The lesion size was defined as the maximum diameter on 3 T DCE MRI. All the statistical analysis was performed in IBM SPSS Statistics (Armonk, NY).

Results

Twenty-eight lesions with an average size of 24 ± 16 mm (range 8–66 mm) were identified in 28 patients (Table 2). The diameter of benign lesions was not significantly different from that of malignant lesions (malignant, 25 ± 17 mm; benign, 22 ± 14 mm [$p=0.62$]). There were 18 malignant and 10 benign lesions. Malignant cases consisted of 15 invasive ductal carcinomas (IDC) (two grade 1, five grade 2, eight grade 3), two invasive lobular carcinomas (ILC) grade 2 and one ductal carcinoma in situ (DCIS). Of the benign lesions, there were eight fibroadenomas, one intraductal papilloma and one case of mastitis.

At 3 T and 7 T, DWI was acquired with high SNR and diagnostic image quality in all patients in clinically acceptable measurement times of 2:56 min (3 T) and 3:48 min (7 T). Figure 1 shows bilateral DWI breast images of a 61-year-old woman acquired at 3 T (left) and 7 T (right), with an IDC (grade 3) in the right breast. Compared to 3 T, the MRI

Table 2 Characteristics of 28 breast lesions in 28 patients arranged according to the BI-RADS classification

Patient no.	Age (years)	Menopausal status	BI-RADS	Tumour type	Tumour size (mm)	Histological type	Verification
1	63	Post	5	Malignant	66	IDC/G3	Surgery
2	61	Post	5	Malignant	57	IDC/G3	Surgery
3	81	Post	5	Malignant	53	IDC/G3	Surgery
4	72	Post	5	Malignant	39	IDC/G3	Surgery
5	67	Post	5	Malignant	13	IDC/G3	Surgery
6	45	Pre	5	Malignant	21	IDC/G3	Surgery
7	62	Post	5	Malignant	14	IDC/G3	Surgery
8	52	Post	5	Malignant	25	IDC/G3	Surgery
9	68	Post	5	Malignant	36	IDC/G2	Surgery
10	45	Pre	5	Malignant	22	IDC/G2	Surgery
11	69	Post	5	Malignant	17	IDC/G2	Surgery
12	54	Post	5	Malignant	16	IDC/G2	Surgery
13	74	Post	5	Malignant	15	IDC/G2	Surgery
14	72	Post	5	Malignant	8	ILC/G2	Surgery
15	69	Post	5	Malignant	10	ILC/G2	Surgery
16	63	Post	4	Malignant	16	IDC/G1	Surgery
17	72	Post	4	Malignant	10	IDC/G1	Surgery
18	31	Pre	4	Benign	25	FA	Biopsy
19	55	Post	4	Malignant	20	DCIS	Surgery
20	50	Post	4	Benign	22	FA	Biopsy
21	45	Pre	4	Benign	17	FA	Biopsy
22	34	Pre	4	Benign	13	FA	Biopsy
23	33	Pre	4	Benign	12	FA	Biopsy
24	41	Pre	4	Benign	11	FA	Biopsy
25	69	Post	4	Benign	16	Papilloma	Biopsy
26	23	Pre	3	Benign	45	FA	Follow-up
27	31	Pre	3	Benign	50	Mastitis	Biopsy
28	33	Post	3	Benign	11	FA	Follow-up

IDC invasive ductal carcinoma, ILC invasive lobular carcinoma, FA fibroadenoma, G1–G3 grades 1–3

acquired at 7 T had a 2.4-fold higher spatial resolution (9.8/4.1 mm³ at 3 T/7 T), with higher contrast and more detailed information.

Figures 2 and 3 show examples of DWI in benign lesions. Figure 3 depicts bilateral contrast-enhanced imaging compared to DWI, without diffusion weighting in a benign fibroadenoma of a 31-year-old patient. Fat suppression was good over the whole image at both field strengths. Notice the DWIs measured with $b=0$ s/mm² showing T₂-weighted contrast and high anatomical details.

There was no significant difference between SNR at 3 T and 7 T (malignant, $p=0.677$; benign, $p=0.704$) and there was no significant difference between CNR of benign ($p=0.320$) and malignant ($p=0.435$) lesions at 3 T and 7 T. In particular the mean SNR was 66.3±25.3/51.0±17.4, 65.5±19.5/52.6±18.1 and 28.0±12.1/21.0±9.75 in benign lesions, malignant lesions and healthy tissue at 3 T/7 T. SNR values from healthy tissue on the contralateral breast were found to be 30.0±12.2/

23.1±11.2 in the para-mammillar area, 28.3±11.2/21.5±9.7 in the central area and 25.7±12.8/18.5±7.9 in the pre-pectoral area (3 T/7 T). This indicates decreasing SNR towards the pre-pectoral area. Average CNR values for benign lesions were 2.69±1.13/3.29±0.92 and 3.31±1.11/3.60±1.64 for malignant lesions at 3 T/7 T.

A comparison of the ADC values is shown in a box plot (Fig. 4). A Bland–Altman plot (Fig. 5) shows good agreement between the ADC values at 3 T and 7 T. However, the ADC values were significantly lower at 7 T than that at 3 T. The average ADC values were 1.73±0.28×10⁻³/1.64±0.29×10⁻³ mm²/s in healthy tissue ($p=0.005$), 1.66±0.40×10⁻³/1.60±0.38×10⁻³ mm²/s ($p=0.03$) in benign lesions and 0.86±0.15×10⁻³/0.70±0.17×10⁻³ mm²/s in malignant lesion ($p<0.001$) at 3 T and 7 T, respectively. The mean difference of ADC values between the two field strengths was twice as low in healthy tissue than in malignant lesions (see Fig. 5).

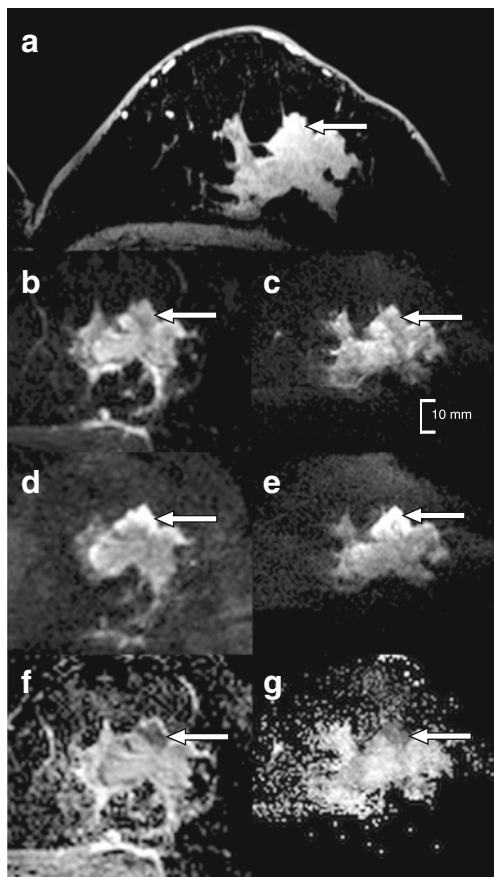


Fig. 1 An example of a malignant breast lesion in a 61-year-old woman with an IDC (grade 3) depicted on contrast-enhanced and DWI images at 3 T (left) and 7 T (right). **a** Contrast-enhanced T_1 -weighted image at 7 T; DWI images with **b**, **c** $b=0$ s/mm² and **d**, **e** $b=850$ s/mm²; **f**, **g** ADC maps

An ADC threshold of 1.275×10^{-3} mm²/s [27] differentiated benign and malignant breast lesions with a sensitivity of 94 % (95 % CI 73–99 %), a specificity of 90.00 % (95 % CI 55–98 %), a PPV of 94 % (95 % CI 73–99 %) and an NPV of 90 % (95 % CI 55–98 %) at 3 T. There were 17 true-positive, nine true-negative, one false-positive and one false-negative lesion at 3 T. At 7 T, the same ADC threshold identified 18 lesions as true-positive, nine as true-negative, and one as false-positive, leading to a higher sensitivity of 100 % (95 % CI 81–100 %), a specificity of 90 % (95 % CI 55–98 %), a PPV of 95 % (95 % CI 74–99 %) and an NPV of 100 % (95 % CI 66–100 %).

Note that we used the ADC threshold which was based on a higher number of patients but with different b values (this work: 0, 850 mm²/s; literature value: 50, 850 mm²/s) [27]. Therefore, we calculated the ADC thresholds for 3 T and 7 T using ROC analysis. This did not further improve the diagnostic accuracy.

The false-positive case at both 3 T and 7 T was mastitis. The false-negative case at 3 T was a grade 2 IDC which had a reported diameter of 17 mm on DCE MRI.

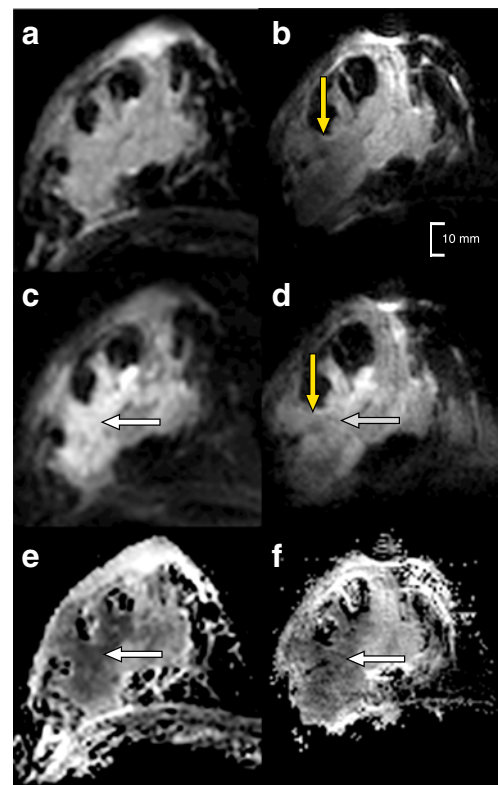


Fig. 2 DWI images of a patient (age 31 years) with benign mastitis in the right breast at 3 T (left) and 7 T (right). DWIs with **a**, **b** $b=0$ s/mm² and **c**, **d** $b=850$ s/mm²; **e**, **f** ADC maps. White arrows indicate the lesion, which is characterised by hyperintense signal on DWI ($b=850$ s/mm²) and hypointensity on ADC maps. Yellow arrows point to the loss of signal on DWI images at 7 T in comparison with 3 T images

Discussion

This study comparing bilateral DWI in breast cancer patients at 3 T and 7 T demonstrates the potential of 7 T DWI for breast lesions diagnosis. At both field strengths, images were acquired without significant artefacts and with satisfactory fat suppression, resulting in a high specificity of 90 % at both field strengths and a sensitivity of 94.4 % and 100 % at 3 T and 7 T, respectively, on the basis of an ADC threshold of 1.275×10^{-3} mm²/s.

There were no significant differences in CNR or SNR between 3 T and 7 T, but the spatial resolution was 2.4-fold higher at 7 T than at 3 T. The in-plane resolution was altered with the ratio of the magnetic field strengths. We have chosen this simple assumption to give a qualitative impression of high-resolution DWI at 7 T which was, therefore, acquired with a sub-millimetre in-plane resolution comparable to that of clinical DCE images at lower field strengths.

At 1.5 T and 3 T, most DWI studies of the breast were performed using ss-EPI, which is prone to image artefacts (i.e. ghosting artefacts, geometric distortions, T_2^* image blurring) that are even more profound at higher field strengths [11, 21, 28, 29]. Strong T_2^* blurring, in particular at 7 T, prevents the anticipated increase in spatial resolution. This limits the diagnostic power of

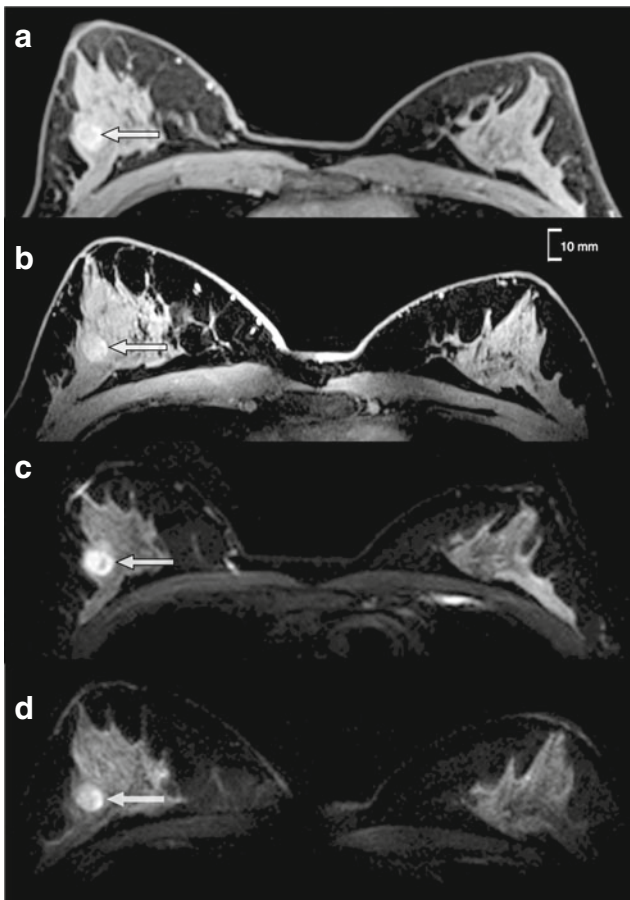


Fig. 3 An example of bilateral DCE MRI (a 3 T, b 7 T) compared to DWI images (c 3 T, d 7 T) without diffusion weighting ($b=0 \text{ s/mm}^2$) of a benign fibroadenoma in the right breast (patient’s age 31 years). The lesions are bright on the rs-EPI images with $b=0 \text{ s/mm}^2$ owing to an increased extracellular water content which is reflected by high ADC values. There is a slight signal loss in the axillary area on the 7 T image

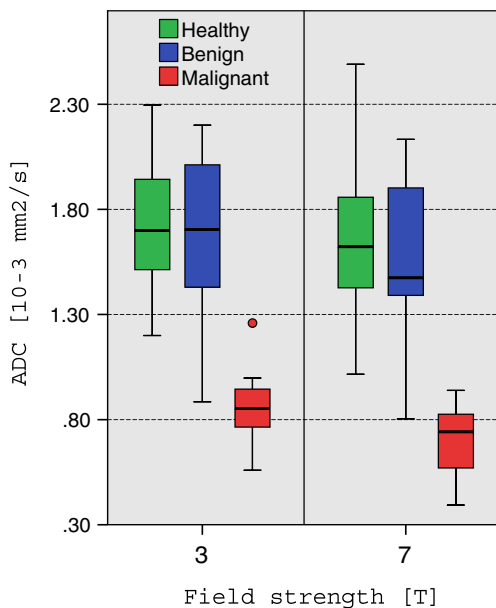


Fig. 4 Comparison of the ADC values measured at 3 T and 7 T. The false-negative case (IDC, grade 2) on 3 T was true-positive on 7-T ADC maps

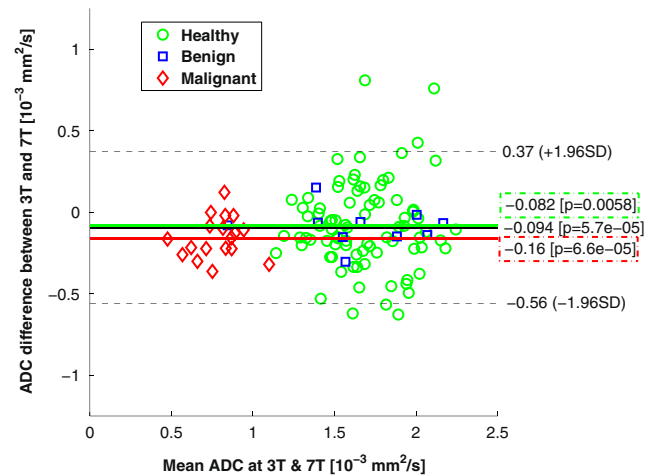


Fig. 5 The Bland–Altman plot illustrates slightly lower ADC values measured at 7 T. No systematic error could be seen in the evaluation between ADC values measured at 3 and 7 T. There was one false-positive case found at both field strengths. The mean differences between ADC values measured at 3 T and 7 T are calculated separately for all data together (solid black line), healthy tissue only (green line, green boxed value) and malignant tissue only (red line, red boxed value)

ss-EPI-based DWI. Korteweg et al. showed preliminary and promising unilateral breast-DWI results using ss-EPI, but the spatial resolution and image quality were hampered by the use of ss-EPI, fat suppression failure and motion artefacts [9, 19]. This resulted in an in-plane resolution of 2 mm in their 7 T breast DWI, compared to 0.9 mm, which was used in this study. In a comparison between ss-EPI and rs-EPI in breast DWI at 3 T, a threefold reduction of geometric distortions and significantly improved diagnostic accuracy were reported using rs-EPI compared to ss-EPI [11]. Van de Bank et al. used parallel imaging (PI) at 7 T to increase the spatial/temporal resolution of DCE MRI and to decrease geometric distortions in breast-DWI at 7 T. [20, 30]. At 7 T, we combined rs-EPI with PI to further reduce the geometric distortions as recently shown by Bogner et al [23]. This resulted in breast DWI without significant artefacts, satisfactory fat suppression and high diagnostic accuracy based on ADC quantification.

Few studies have compared DCE breast MRI or breast DWI between 7 T and lower field strengths. In a pilot study with a 10-cm-diameter single-loop coil on healthy volunteers and five patients with breast cancer, 2.8–3.8 times higher SNRs were reported in breast MRI at 7 T, when compared to 1.5 T [31]. Korteweg et al. reported a 5.7-fold SNR increase at 7 T compared to 3 T in breast MRI [9, 19]. Gruber et al. did a direct comparison between 3 T and 7 T of 24 patients who underwent breast DCE MRI [9]. They found comparable SNR between 3 T and 7 T, but used spatial resolution at 7 T was 3.2 times higher than at 3 T. In this study, the SNR at 3 T and 7 T was comparable, but the spatial resolution was 2.4-fold higher, resulting in DWI with sub-millimetre in-plane resolution at 7 T.

The high diagnostic accuracy at 3 T and 7 T in this study is based on an ADC threshold of $1.275 \times 10^{-3} \text{ mm}^2/\text{s}$, established

previously in a larger patient study ($n=247$ patients) at 3 T [27]. The ADC values, measured in this study at 3 T, are in agreement with values reported previously. ADC values at 7 T were 4–22 % lower than those at 3 T. Differences between ADC values at different field strengths have been reported previously in the liver and the brain [32, 33]. Dale et al. found higher ADC values in the liver at 3 T, when compared to those at 1.5 T. They did not find any differences between 1.5 T and 3 T in the pancreas [32, 33]. On the other hand, lower ADC values in the brain were reported at 3 T, when compared to 1.5 T [32, 33]. It is not expected that field strength per se is changing the determined ADC values, but other relevant hardware differences may exist. Also, recent papers concluded that higher spatial resolution in breast DWI may lead to lower ADCs particularly in small malignant lesions owing to reduced partial volume effects [34, 35]. This is in agreement with the findings of this study. The mean difference of ADC values between 3 T and 7 T in malignant lesions was twice as high as in healthy tissue. Other authors pointed out that in addition to the spatial resolution other parameters such as magnetic susceptibility, SNR and the fat suppression performance may alter the ADC values [36, 37].

This study has several limitations. We used a high in-plane resolution but a relatively large slice thickness of 5 mm. Frost et al. proposed rs-EPI with multislice acceleration to reduce scan time for DWI at 3 and 7 T [38]. Such a sequence allows one to acquire either thinner slices or to decrease TR to optimize SNR per unit time. In addition, results of this study could be affected by ROI misregistration between 3 T and 7 T. Furthermore, larger studies should be conducted including smaller tumours to evaluate potential advantages of 7 T DWI to resolve smaller anatomical structures. The method for SNR quantification used with parallel imaging may affect SNR calculation. We used a dual-tuned, bilateral $^1\text{H}/^{31}\text{P}$ breast coil at 7 T. A single-tuned coil, optimized for proton imaging would, therefore, further improve the SNR obtained for breast MRI at 7 T. A reduced B_1^+ field in the pre-pectoral region and the lateral region, compared to the central region of the breast, was reported at 7 T [9]. This results in reduced SNR in T_1 -w images at 7 T, which was reported in several studies [9, 19, 20, 31, 39]. ADC maps are less sensitive to B_1 heterogeneities, because they are calculated from two images with the same B_1 errors. Nevertheless, DWI in such regions can be biased as a result of a T_2 black-out effect in regions with low SNR. In addition, this hampers the overall image quality of the $b=0$ s/mm^2 DWI images limiting the use for morphological assessment of lesions and healthy tissue. Current developments of MRI technology, in particular, advanced B_1^+ shimming technology provided by multi-transmit hardware [40], will further improve breast DWI at 7 T.

In this study 7 T DWI versus 3 T DWI resulted in increased sensitivity, but not specificity. We had one false-positive

(mastitis, at 3 T and 7 T) and one false-negative (IDC grade 2, at 3 T only) case. Interestingly, the false-negative finding at 3 T was very small (a 17-mm diameter reported on DCE MRI; however, it had a less than 10-mm diameter on DWI and it was visible only on one DWI slice at both 3 and 7 T). At 7 T, the lesion was identified correctly. This motivates us to conduct further studies that would include lesions that are more difficult to diagnose, in particular small lesions and non-mass-like enhancing lesions.

Our results suggest that 7 T DWI of the breast can be performed with significantly higher spatial resolution (2.4-fold) than that at 3 T, without significant differences in SNR.

Acknowledgments The scientific guarantor of this publication is Stephan Gruber. The authors of this manuscript declare no relationships with any companies whose products or services may be related to the subject matter of the article. This study has received funding by Austrian Nationalbank ‘Jubiläumfond’ Project No. 13418 and 15082. No complex statistical methods were necessary for this paper. Institutional review board approval was obtained. Written informed consent was obtained from all subjects (patients) in this study. Some study subjects or cohorts have been previously reported in (1) Dynamic contrast-enhanced magnetic resonance imaging of breast tumors at 3 and 7 T: a comparison. *Investigative Radiology* 2014; (2) Clinical application of bilateral high temporal and spatial resolution dynamic contrast-enhanced magnetic resonance imaging of the breast at 7 T. *European Radiology* 2014; (3) Bilateral diffusion-weighted MR imaging of breast tumors with submillimeter resolution using readout-segmented echo-planar imaging at 7 T. Methodology: prospective, diagnostic or prognostic study, performed at one institution.

References

1. Boetes C, Veltman J, van Die L, Bult P, Wobbes T, Barentsz JO (2004) The role of MRI in invasive lobular carcinoma. *Breast Cancer Res Treat* 86:31–37
2. Kinkel K, Helbich TH, Esserman LJ et al (2000) Dynamic high-spatial-resolution MR imaging of suspicious breast lesions: diagnostic criteria and interobserver variability. *AJR Am J Roentgenol* 175:35–43
3. Schnall MD, Blume J, Bluemke DA et al (2006) Diagnostic architectural and dynamic features at breast MR imaging: multicenter study. *Radiology* 238:42–53
4. Davis PL, McCarty KS Jr (1997) Sensitivity of enhanced MRI for the detection of breast cancer: new, multicentric, residual, and recurrent. *Eur Radiol* 7:289–298
5. Orel SG, Schnall MD (2001) MR imaging of the breast for the detection, diagnosis, and staging of breast cancer. *Radiology* 220: 13–30
6. Heywang-Kobrunner SH, Viehweg P, Heinig A, Kuchler C (1997) Contrast-enhanced MRI of the breast: accuracy, value, controversies, solutions. *Eur J Radiol* 24:94–108
7. Kuhl C (2007) The current status of breast MR imaging. Part I. Choice of technique, image interpretation, diagnostic accuracy, and transfer to clinical practice. *Radiology* 244:356–378
8. Benndorf M, Baltzer PA, Vag T, Gajda M, Runnebaum IB, Kaiser WA (2010) Breast MRI as an adjunct to mammography: Does it really suffer from low specificity? A retrospective analysis stratified by mammographic BI-RADS classes. *Acta Radiol* 51:715–721

9. Gruber S, Pinker K, Zaric O et al (2014) Dynamic contrast-enhanced magnetic resonance imaging of breast tumors at 3 and 7 T: a comparison. *Invest Radiol* 49:354–362
10. Bogner W, Gruber S, Pinker K et al (2009) Diffusion-weighted MR for differentiation of breast lesions at 3.0 T: how does selection of diffusion protocols affect diagnosis? *Radiology* 253:341–351
11. Bogner W, Pinker-Domenig K, Bickel H et al (2012) Readout-segmented echo-planar imaging improves the diagnostic performance of diffusion-weighted MR breast examinations at 3.0 T. *Radiology* 263:64–76
12. Pinker K, Bogner W, Baltzer P et al (2014) Improved diagnostic accuracy with multiparametric magnetic resonance imaging of the breast using dynamic contrast-enhanced magnetic resonance imaging, diffusion-weighted imaging, and 3-dimensional proton magnetic resonance spectroscopic imaging. *Invest Radiol* 49:421–430
13. Stadlbauer A, Bernt R, Gruber S et al (2009) Diffusion-weighted MR imaging with background body signal suppression (DWIBS) for the diagnosis of malignant and benign breast lesions. *Eur Radiol* 19:2349–2356
14. Hahn SY, Ko EY, Han BK, Shin JH, Ko ES (2014) Role of diffusion-weighted imaging as an adjunct to contrast-enhanced breast MRI in evaluating residual breast cancer following neoadjuvant chemotherapy. *Eur J Radiol* 83:283–288
15. Spick C, Pinker-Domenig K, Rudas M, Helbich TH, Baltzer PA (2014) MRI-only lesions: application of diffusion-weighted imaging obviates unnecessary MR-guided breast biopsies. *Eur Radiol* 24:1204–1210
16. Ladd ME (2007) High-field-strength magnetic resonance: potential and limits. *Top Magn Reson Imaging* 18:139–152
17. Matsuoka A, Minato M, Harada M et al (2008) Comparison of 3.0- and 1.5-tesla diffusion-weighted imaging in the visibility of breast cancer. *Radiat Med* 26:15–20
18. Trattnig S, Zbyn S, Schmitt B et al (2012) Advanced MR methods at ultra-high field (7 Tesla) for clinical musculoskeletal applications. *Eur Radiol* 22:2338–2346
19. Korteweg MA, Veldhuis WB, Visser F et al (2011) Feasibility of 7 Tesla breast magnetic resonance imaging determination of intrinsic sensitivity and high-resolution magnetic resonance imaging, diffusion-weighted imaging, and (1)H-magnetic resonance spectroscopy of breast cancer patients receiving neoadjuvant therapy. *Invest Radiol* 46:370–376
20. van de Bank BL, Voogt IJ, Italiaander M et al (2012) Ultra high spatial and temporal resolution breast imaging at 7 T. *NMR Biomed*. doi:10.1002/nbm.2868
21. Holdsworth SJ, Skare S, Newbould RD, Bammer R (2009) Robust GRAPPA-accelerated diffusion-weighted readout-segmented (RS)-EPI. *Magn Reson Med* 62:1629–1640
22. Heidemann RM, Porter DA, Anwender A et al (2010) Diffusion imaging in humans at 7 T using readout-segmented EPI and GRAPPA. *Magn Reson Med* 64:9–14
23. Bogner W, Pinker K, Zaric O et al (2015) Bilateral diffusion-weighted MR imaging of breast tumors with submillimeter resolution using readout-segmented echo-planar imaging at 7 T. *Radiology* 274:74–84
24. Sardanelli F, Boetes C, Borisch B et al (2010) Magnetic resonance imaging of the breast: recommendations from the EUSOMA working group. *Eur J Cancer* 46:1296–1316
25. McLaughlin RL, Newitt DC, Wilmes LJ et al (2014) High resolution in vivo characterization of apparent diffusion coefficient at the tumor-stromal boundary of breast carcinomas: a pilot study to assess treatment response using proximity-dependent diffusion-weighted imaging. *J Magn Reson Imaging* 39:1308–1313
26. Pinker K, Bogner W, Baltzer P et al (2014) Clinical application of bilateral high temporal and spatial resolution dynamic contrast-enhanced magnetic resonance imaging of the breast at 7 T. *Eur Radiol* 24:913–920
27. Pinker K, Bickel H, Helbich TH et al (2013) Combined contrast-enhanced magnetic resonance and diffusion-weighted imaging reading adapted to the “Breast Imaging Reporting and Data System” for multiparametric 3-T imaging of breast lesions. *Eur Radiol* 23:1791–1802
28. Baltzer PA, Renz DM, Herrmann KH et al (2009) Diffusion-weighted imaging (DWI) in MR mammography (MRM): clinical comparison of echo planar imaging (EPI) and half-Fourier single-shot turbo spin echo (HASTE) diffusion techniques. *Eur Radiol* 19:1612–1620
29. Porter DA, Heidemann RM (2009) High resolution diffusion-weighted imaging using readout-segmented echo-planar imaging, parallel imaging and a two-dimensional navigator-based reacquisition. *Magn Reson Med* 62:468–475
30. Kuroki Y, Nasu K, Kuroki S et al (2004) Diffusion-weighted imaging of breast cancer with the sensitivity encoding technique: analysis of the apparent diffusion coefficient value. *Magn Reson Med* 53:79–85
31. Umutlu L, Maderwald S, Kraff O et al (2010) Dynamic contrast-enhanced breast MRI at 7 Tesla utilizing a single-loop coil: a feasibility trial. *Acad Radiol* 17:1050–1056
32. Dale BM, Braithwaite AC, Boll DT, Merkle EM (2010) Field strength and diffusion encoding technique affect the apparent diffusion coefficient measurements in diffusion-weighted imaging of the abdomen. *Invest Radiol* 45:104–108
33. Huisman TA, Loenneker T, Barta G et al (2006) Quantitative diffusion tensor MR imaging of the brain: field strength related variance of apparent diffusion coefficient (ADC) and fractional anisotropy (FA) scalars. *Eur Radiol* 16:1651–1658
34. Wisner DJ, Rogers N, Deshpande VS et al (2013) High-resolution diffusion-weighted imaging for the separation of benign from malignant BI-RADS 4/5 lesions found on breast MRI at 3 T. *J Magn Reson Imaging*. doi:10.1002/jmri.24416
35. Wilmes LJ, McLaughlin RL, Newitt DC et al (2013) High-resolution diffusion-weighted imaging for monitoring breast cancer treatment response. *Acad Radiol* 20:581–589
36. Woodhams R, Matsunaga K, Iwabuchi K et al (2005) Diffusion-weighted imaging of malignant breast tumors: the usefulness of apparent diffusion coefficient (ADC) value and ADC map for the detection of malignant breast tumors and evaluation of cancer extension. *J Comput Assist Tomogr* 29:644–649
37. Nogueira L, Brandao S, Nunes RG, Ferreira HA, Loureiro J, Ramos I (2015) Breast DWI at 3 T: influence of the fat-suppression technique on image quality and diagnostic performance. *Clin Radiol* 70:286–294
38. Frost R, Jezzard P, Douaud G, Clare S, Porter DA, Miller KL (2014) Scan time reduction for readout-segmented EPI using simultaneous multislice acceleration: diffusion-weighted imaging at 3 and 7 Tesla. *Magn Reson Med*. doi:10.1002/mrm.25391
39. Stehouwer BL, Klomp DW, Korteweg MA et al (2013) 7 T versus 3 T contrast-enhanced breast magnetic resonance imaging of invasive ductal lobular carcinoma: first clinical experience. *Magn Reson Imaging* 31:613–617
40. Wu X, Akgun C, Vaughan JT et al (2010) Adapted RF pulse design for SAR reduction in parallel excitation with experimental verification at 9.4T. *J Magn Reson*. doi:10.1016/j.jmr.2010.04.018